Volume: 12 Issue: 06 Pages: 4732-4741(2021) ISSN: 0975-0290

# Control Strategies for DFIG based Wind Turbine Systems Frequency Regulating

**Jamshed Ali Shaikh**
Dept. of State Key Laboratory of Power Transmission, Chongqing University, Chongqing, China.
Email: jamshed@cqu.edu.cn
**Umer Farooq**
Dept. of State Key Laboratory of Power Transmission, Chongqing University, Chongqing, China
Email: umerfarooq.cqu@yahoo.com
**Muhammad Shoaib Bhutta**
Email: shoaibbhutta@hotmail.com
Dept. of State Key Laboratory of Power Transmission, Chongqing University, Chongqing, China

**ABSTRACT**

**As the energy crisis worsens and global problems intensify, wind power generation has emerged as one of the most successful and fastest-growing alternatives among some of the different mechanisms. The running of a power plant is continually jeopardized by irregular and malfunctioning circumstances. A conceptual implementation of an innovative solution is suggested for the proper output of a wind turbine power system in a wind-solar hybrid microgrid to track frequency fluctuations caused by various load factors and environmental conditions (MG). As a standard PI controller is used to track frequency, it is coupled with a sophisticated fuzzy logic controller to enhance frequency regulation. The frequency response properties of traditional WTs are tested and distinguished with varying loads and wind speeds. It is claimed that as the wind power speed rises, the power output of the device would deteriorate. The simulation shows that frequency modulation is accomplished in the time allocated. Furthermore, the proposed solution can be implemented into day-to-day applications without making any external modifications.**

Keywords - **DFIG, PI traditional controller, Droop control coefficient, Inertia control coefficient**

Date of Submission: Apr 26, 2021 Date of Acceptance: May 17, 2021

## I. INTRODUCTION

Due to its high significant and varied financial development role, renewable energy has risen in importance in today's advanced society. Due to the extreme ongoing fast expansion of wind power into power grids, a few international countries, including Austria, Germany, and Denmark, have run out of viable locations for onshore wind power projects due to high population density. Furthermore, offshore wind energy supplies have been shown to be much higher than onshore wind energy capabilities. As a consequence, offshore wind turbines have enormous capacity as large-scale, sustainable electric power sources. The use of a doubly fed induction generator (DFIG) has risen significantly over the last 15 years [1, 2].

Wind power's explosive development in Europe, and more recently in the United States and China, has altered the way Transmission System Operators (TSOs) handle electricity grids [3, 4]. However, in offshore wind farms, the distance between the wind turbines and the sea is much greater than in onshore wind farms. As a consequence, in contrast to onshore wind farms, where the voltage level of the wind farm is usually the same as the voltage degree of the transmission device, offshore wind farms require higher voltage degrees with reliable and efficient transmitting strains to minimize strength losses. In the arena, many major offshore wind turbines are now operating. Future offshore wind farm tasks could be larger and further from the shore [5].

Since the majority of wind turbines use induction turbines to control digital devices (DFIG wind turbines), the phenomenon was initially related to self-excitation caused by induction generator effects (IGE). According to the following appraisal [6, 7], the main object of the interaction had to be tracked back to the interaction between the controller of the wind turbine converters and the transmission line.

When the rotor is moved at a variable velocity, the doubly-fed induction generator driven by a Wind Turbine generates a hard and quick frequency voltage from the stator windings without issue, and the excitation control electronics converter feeding the rotor windings may be valued at a fraction of the nominal value. In recent years, wind turbines focused on the doubly fed induction generator (DFIG) have become more popular in massive wind farms [9, 11]. The growing number of DFIGs linked to the electric grid is primarily due to low converter intensity ratings and the capacity to supply output at constant voltage and frequency as rotor speed varies [12].

The DFIG theorem also allows for the control of the total power factor of the machine. The bulk of large-capacity devices (>1 MW) are electric-Wind [13].

Strength digital converters may be used to monitor the generator's operating characteristics, such as speed and reactive capacity [14, 15]. A wind turbine may be operated in one of two ways. The key objective is to keep the

Volume: 12 Issue: 06 Pages: 4732-4741(2021) ISSN: 0975-0290

rotational speed reasonably constant, such that a surge in wind velocity just marginally raises the rotor velocity above the synchronous rate, allowing the slip to differ [16, 17].

This is mostly concerned with the torque-pace relationship of an induction motor. A pace monitor is used to adjust the pitch of the blades at high wind levels to minimize energy consumption and secure the wind turbine. by using a time interval defined as the tip speed ratio [18].

As a consequence, we investigate the frequency control approach utilized by DFIG WTs, which has a direct effect on the development of the WTs power system industry. The frequency accuracy of the power grid is important for the system's unit reliability to achieve the norm. Its significance differs with the system as the active power supply-demand connection changes, and electromotive energy separates it into a rotating magnetic field. If the synchronous generator stator is attached to an asymmetrical load, the frequency flows via the winding of the stator [19]. The graph below illustrates the relationship between speed and frequency.

$$n_{1=} n_r \pm n_2 \quad (1)$$

$$n_{1=} \frac{60 f_1}{n_p} \quad (2)$$

The grid frequency is represented by f1, the rotor excitation current frequency is represented by f2, and the number of pole pairs is represented by np of DFIG.

$$n_{2=} \frac{60 f_2}{n_p} \quad (3)$$

$$f_{2=} \frac{n_p}{60} n_r \pm f_2 \quad (4)$$

The frequency of excitation current to the rotor side under control changes is f2, and the rotor speed of the DFIG is nr at various wind penetrations.

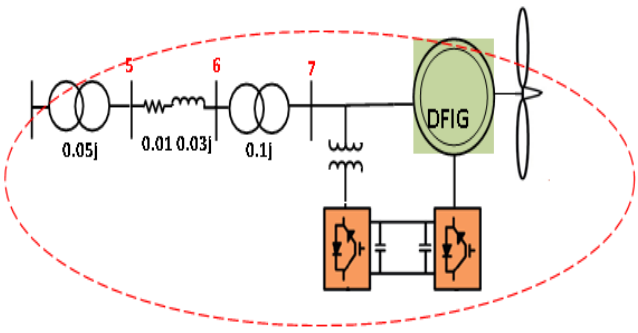


**Fig 1.** Schematic of a DFIG-based wind farm connected to the IEEE first benchmark model

DFIG's device configuration is seen in Figure 1. Electronic power converter control is used to adjust variable speed and constant frequency activity. In order to bind to the grid, the active and reactive electricity must be decoupled. DFIG normally monitors the highest power point, and it makes little reference to the supply and demand power balance since it lacks an appropriate control strategy. With the incorporation of large-scale wind power into the power grid, electricity systems are posing greater frequency stability problems. Synchronous generator turbines change their governors automatically to satisfy frequency regulation requirements; however, wind generators contribute only a limited amount, if any, to frequency stability. As a result, frequency control systems should be created in such a way that the system can maintain frequency variance by internal modification.

Figure 2 depicts the DFIG's step output when the wind speed is increased from 8 to 12 m/s. The timer for each move was set to 15 seconds. The DFIG wind turbine encounters an average wind speed of 8m/s from 0 to 15 seconds while the stator voltage is stable, the reactive strength is negative, the dynamic power is 3.5 MW, the DC-link voltage is constant, and the rotor speed is 1.02g pu. As the wind speed rises from 15s to 30s, DFIG begins to provide active power to the grid and encounters wind speeds of 12m/s. At this time, the stator current begins to rise, the rotor speed steadily increases, the stator voltage remains steady, the DC connection voltage remains constant, the reactive power remains negative, and the rotor speed gradually increases.

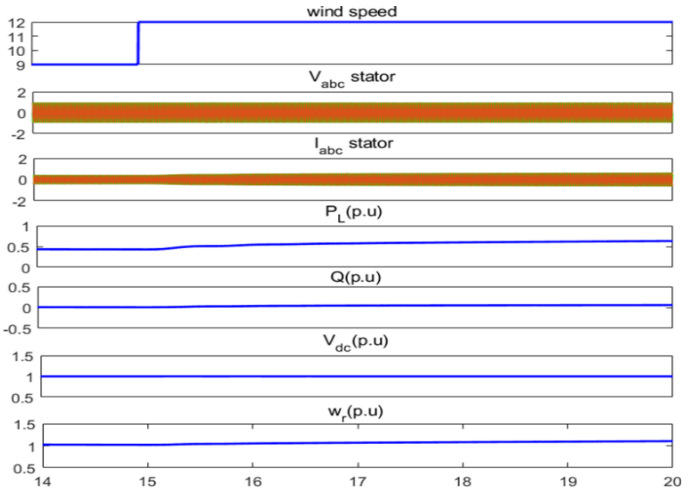


Fig 2. DIFG Response under step change

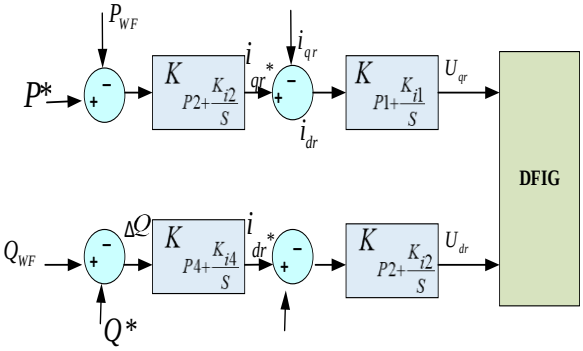


Fig 3. Control block diagram of DFIG rotor side converter

The rotor voltages on the DFIG (q, d) side are (u*rd,, u*rq). P* and Q* are active and reactive control comparison signals, respectively. Kirp, Kirl, Ki1, Ki2, Ki3, Ki4 are the PI gains on the Rotor line. The DFIG (q, d)-side (ird, irq). The DFIG (q, d)-side rotor present comparison values are ird* and irq*.

Volume: 12 Issue: 06 Pages: 4732-4741(2021) ISSN: 0975-0290

$$u_{rd}^{*} = [K_{irP} + \frac{K_{irL}}{s}](i_{rd}^{*} - i_{rd}) + u_{rd}^{'}$$
$$u_{rq}^{*} = [K_{irP} + \frac{K_{irL}}{s}](i_{rq}^{*} - i_{rq}) + u_{rq}^{'} \quad (5)$$

The shaft component is related to the corresponding shaft's rotor current component, where dq is the rotor voltage. As seen in Fig.3, the feedforward compensation concepts Urd and Urq are used to remove coupling components.

For the frequency excursion of the wind energy conversion mechanism, researchers have suggested many approaches. The author suggested a system in which the WT's operating point is shifted between the de-loaded and maximum power point monitoring (MPPT) methods in [20]. The downside of this method was that the droop control benefit was adjusted using an arbitrary pre-defined linear relationship. The author suggested a method using wind power and a vehicle to reflect the power system's frequency stability in [21]. It did not, however, address how wind energy relates to frequency control. The effect of the frequency regulation's droop control gain and inertia control was investigated.

However, the simulation time horizon was insufficient to simulate the wind main reserve reliability [22]. To achieve frequency equilibrium, the author suggested [23] a supervisory control system for a wind farm. [24] looked at the effect of increasing inertia and dormancy control on the frequency regulation guideline's impact.

A novel frequency control for large-scale penetration of WTs is proposed in this paper. The aim of this project is to rapidly diagnose and control frequency abnormalities in order to prevent the device from shutting down completely. The fuzzy logic methodology is combined with a standard PI device to effectively refine the frequency of the machine [25]. Furthermore, this scheme can be used in real-time implementations without any changes.

## II. PROPOSED TECHNIQUE

Due to various their versatility and usefulness for both linear and nonlinear systems, proportional integral (PI) controllers are commonly used in industrial processes, and tuning techniques are still a hot research area to achieve the best controller outcome. To find its parameters, the Proportional Integral (PI) controller is calibrated.

The Fuzzy PI controller, on the other side, does not use the same tuning mechanisms as standard PI controllers. It consists of a large number of control laws and a control signal that are legitimately obtained from the data base and fuzzy inference. Fuzzy sensor parameters are fine-tuned by comparing them to optimal controller values.

The fuzzy-PI controller's output is equivalent to that of a traditional PI controller. The Fuzzy-PI controller outperforms other traditional PI controllers in MATLAB simulations, particularly at higher compensation levels.

In this equation, kd is the inertial control coefficient, kp is the droop control coefficient, e (k) is the error, and e (k) = e(k)-(k- 1) is the difference of the error with unit delay of error.

$$K_p = (K_{p.max} - K_{p.min})K_p' + K_{p.min} \quad (6)$$

$$K_d = (K_{p.max} - K_{p.min})K_p' + K_{p.min} \quad (7)$$

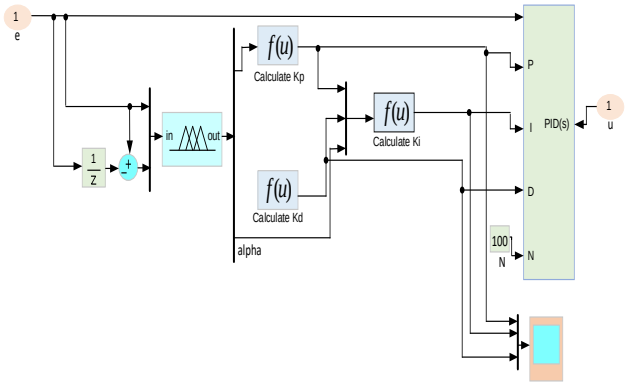


Fig 4. Simulink based Fuzzy logic Controller

The frequency deviation shift limit of the two input amounts is set to [NB, NM, NS, ZO, PS, PM, PB] in the fuzzy sets of the frequency deviation, and the fuzzy set of the fuzzy control link's output is set to [ZO, PS, PM, PB]. Frequency regulation is defined by fuzzy control rules according to the above formulation, and the corresponding control rule is shown in Table I.

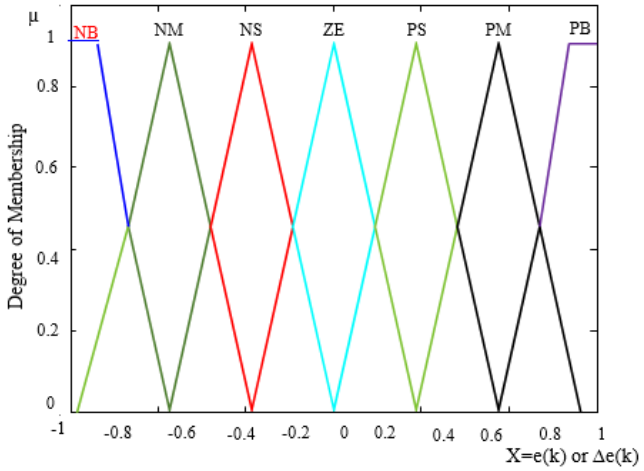


Fig 5. Member ship function for eΔ (k) and Δed(k)

$$\Delta f = E\frac{d\Delta f}{dt}ED \quad (8)$$

with the aid of the equation mentioned in the previous part, as the frequency deviation shift rate ( df)/dt is ED value to the PI controller. FLC updates the input value after each loop to ensure that the signal follows the specified laws. FLC changes its value with each loop of the signal, allowing the function's precise value to be calculated. As we compared both of the results, we discovered that the fuzzy controller is more effective than the conventional controller. Since the fuzzy controller is more precise and takes less time than the standard controller.

When the FLC first starts up, it will check the signal properties. After that, it will choose a value from the table

Volume: 12 Issue: 06 Pages: 4732-4741(2021) ISSN: 0975-0290

based on the rules defined in the membership mechanism of the fuzzy logic controller.

| ED | E | | | | | | |
|---|---|---|---|---|---|---|---|
| | NB | NM | NS | ZE | PS | PM | PB |
| NB | PB | PB | PM | PS | ZO | ZO | ZO |
| NM | PB | PM | PS | PS | ZO | ZO | PS |
| NS | PM | PS | PS | PS | ZO | PS | PS |
| ZO | PS | PS | PS | ZO | PS | PS | PS |
| PS | PS | PS | ZO | PS | PS | PS | PM |
| PM | PS | ZO | ZO | PS | PS | PM | PB |
| PB | ZO | ZO | ZO | PS | PM | PB | PB |

As a result of the rules and logic, calculating the value to use for the particular interval of the signal is easy. The value of the fuzzy logic controller varies for each loop of the signal, allowing the correct value of the operation to be calculated. A three-dimensional model diagram between the input and output can be obtained using the fuzzy control rules in Table I, as seen in fig 5.

To determine the controller's basic value, all three values calculated from the above-mentioned rules are fed into the following equation.

The performance signals from the fuzzy controller are Kp, Kd, and based on the fuzzy controller's laws. On the basis of this data, the values of Kp and Kd are calculated using the number of simulations performed on different processes. For the values, we came up with the following ranges.

$Kp.min = 0.32Ku, \quad Kp.max = 0.6Ku$

$Kd.min = 0.08KuTu, Kd.max = 0.15KuTu$

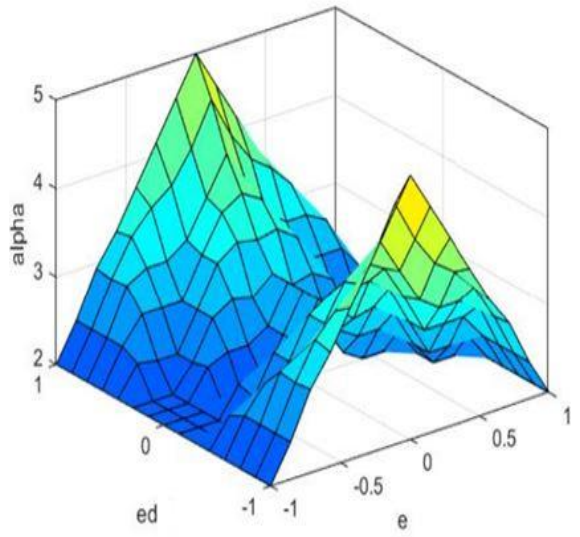


Fig 6. 3D graph of fuzzy logic system

## III. RESULTS & DISCUSSION

To demonstrate the effectiveness of the proposed method approach, it is contrasted to existing techniques: the without-control method, the conventional PI controller method, and the proposed PI controller method with fuzzy reasoning. For frequency modulation, the iteration process optimizes control coefficients (kd, kp). Both techniques are tested at various wind speeds and loads (8 m/s, 9.3 m/s, and 10 m/s), and at different power levels (75 MW, 100 MW, and 125 MW). For simulation, MATLAB is used.

The frequency modulation of DFIG is depicted in Fig. 7-15 using various approaches, including the no-controller system, the standard PI controller method, and the proposed fuzzy logic controller method.

Where figs. 7-9 (a) and (b) represent frequency at 8 m/s with 75MW, 100MW, and 125MW, respectively, and 7-9 (c) represents capacity at 8 m/s with 75MW, 100MW, and 125MW, respectively.

Similarly, fig. 10-12 (a) represents frequency with 75MW, 100MW, and 125MW, fig. 10-12 (b) represents rotor speed with 75MW, 100MW, and 125MW, and fig. 10-12 (c) represents control with 75MW, 100MW, and 125MW.

13-15 (a) represents frequency at 10 m/s with 75MW, 100MW, and 125MW, 13-15 (b) represents rotor speed at 10 m/s with 75MW, 100MW, and 125MW, and 13-15 (c) represents strength at 10 m/s with 75MW, 100MW, and 125MW in the last figure.

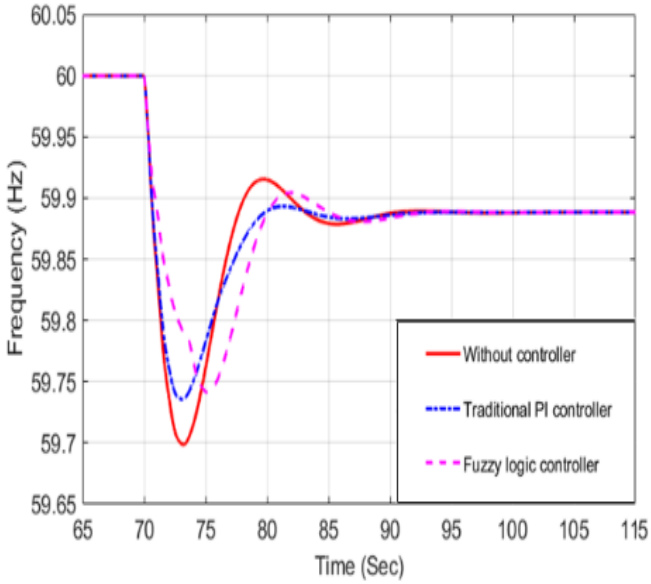


Fig 7. (a) Frequency at 8 m/s with 75MW

Volume: 12 Issue: 06 Pages: 4732-4741(2021) ISSN: 0975-0290

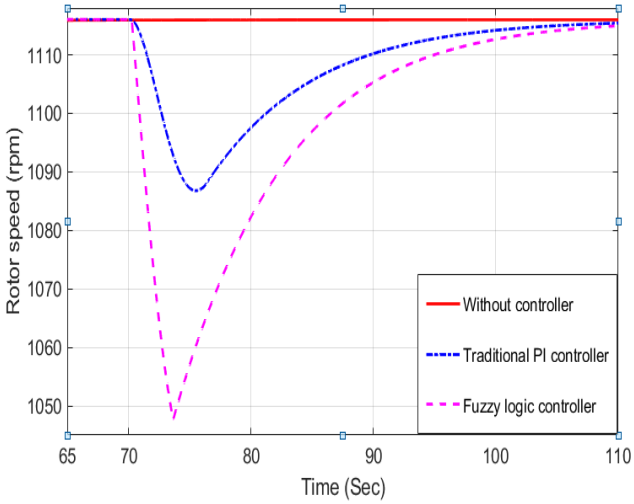


Fig 7. (b) Rotor speed at 8 m/s with 75MW

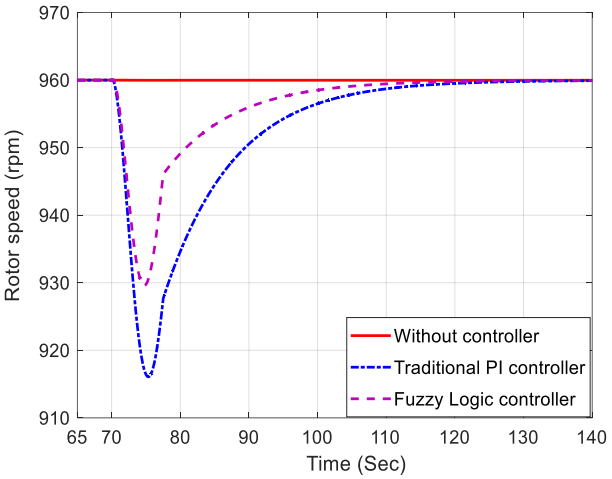


Fig 8. (b) Rotor speed at 8 m/s with 100MW

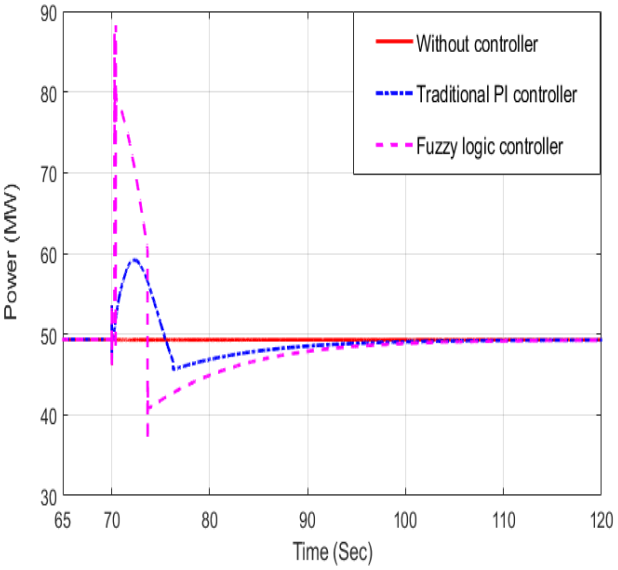


Fig 7. (c) Power at 8 m/s with 75MW

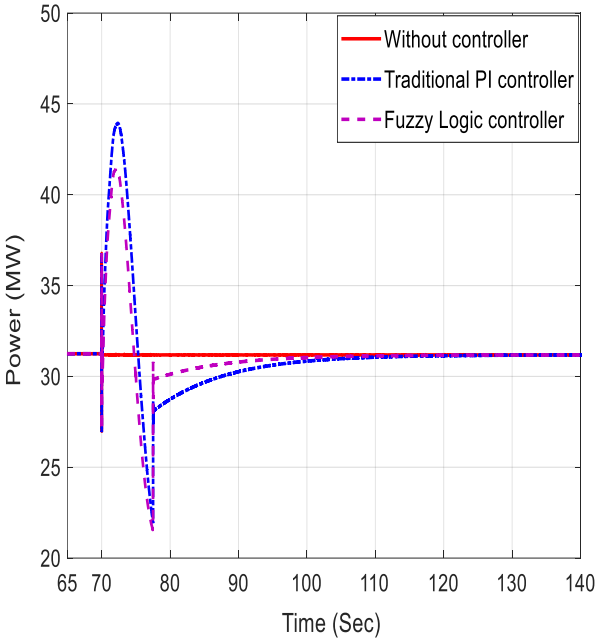


Fig 8. (c) Power at 8 m/s with 100MW

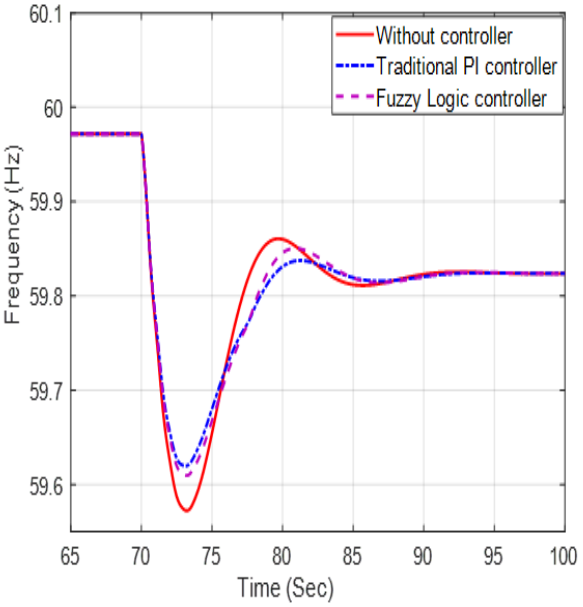


Fig 8. (a) Frequency at 8 m/s with 100MW

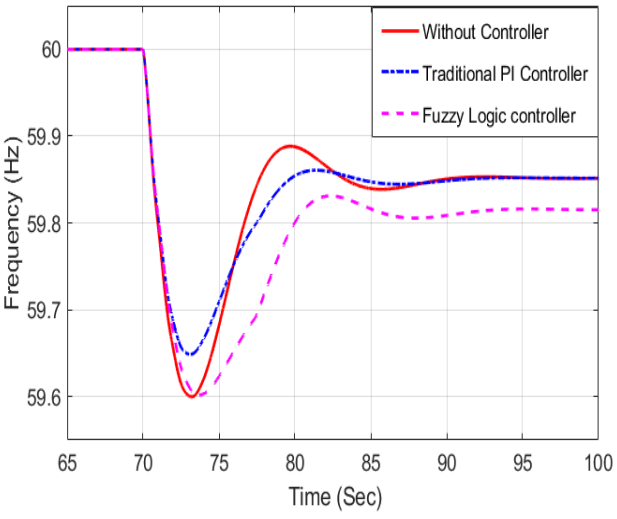


Fig 9. (a) Frequency at 8 m/s with 125MW

Volume: 12 Issue: 06 Pages: 4732-4741(2021) ISSN: 0975-0290

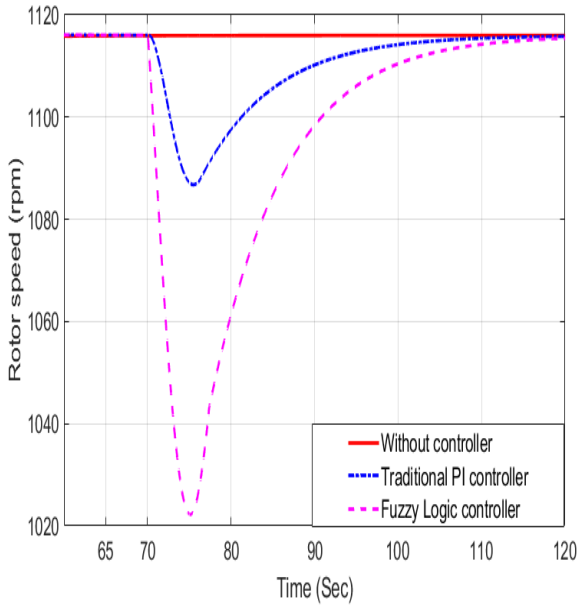


Fig 9. (b) Rotor speed at 8 m/s with 125MW

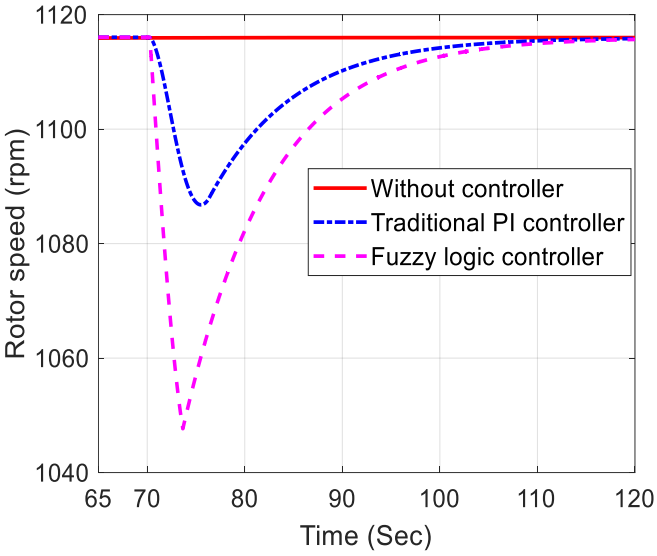


Fig 10. (b) Rotor speed at 9.3 m/s with 75MW

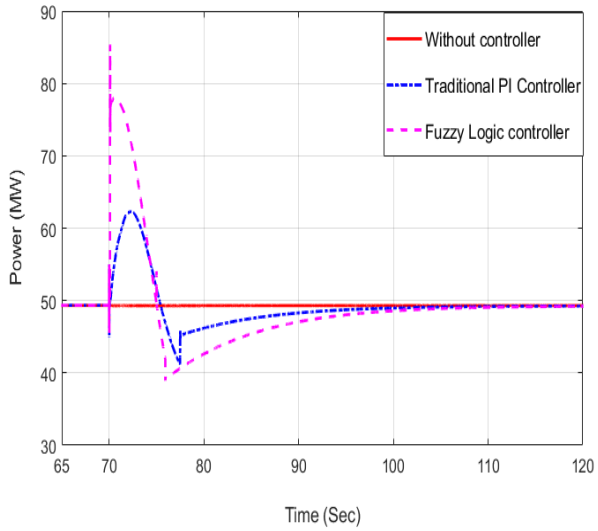


Fig 9. (c) Power at 8 m/s with 125MW

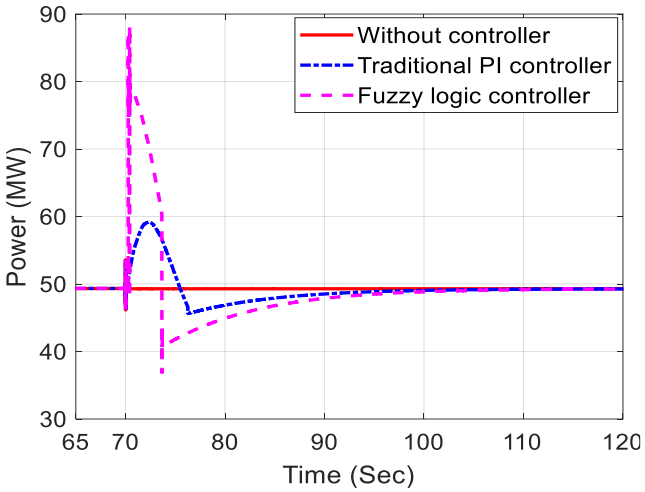


Fig 10. (c) Power at 9.3 m/s with 75MW

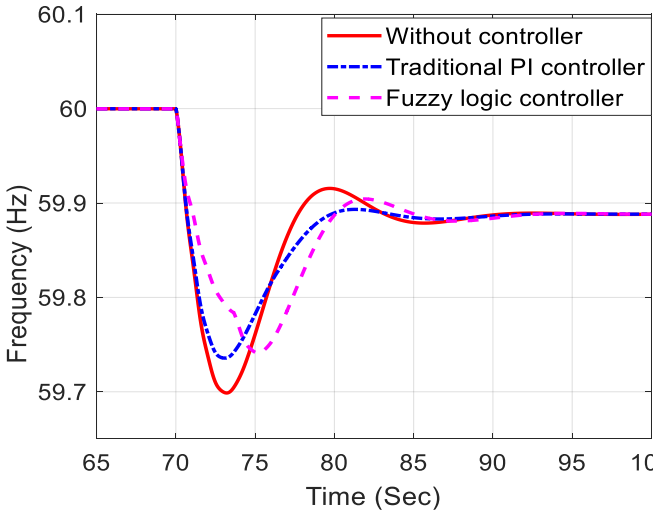


Fig 10. (a) Frequency at 9.3 m/s with 75MW

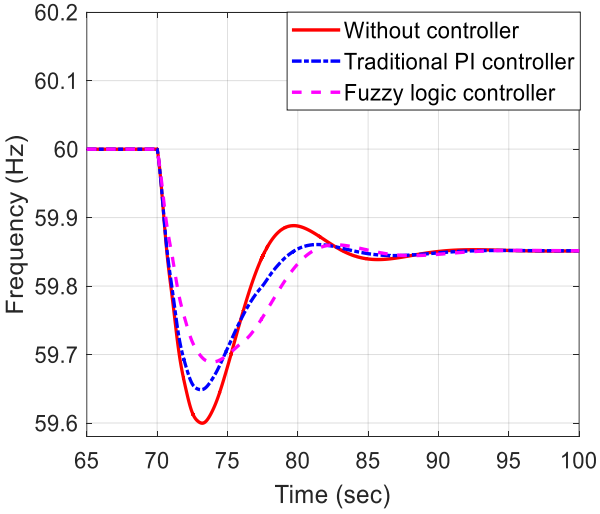


Fig 11. (a) Frequency at 9.3 m/s with 100 MW

Volume: 12 Issue: 06 Pages: 4732-4741(2021) ISSN: 0975-0290

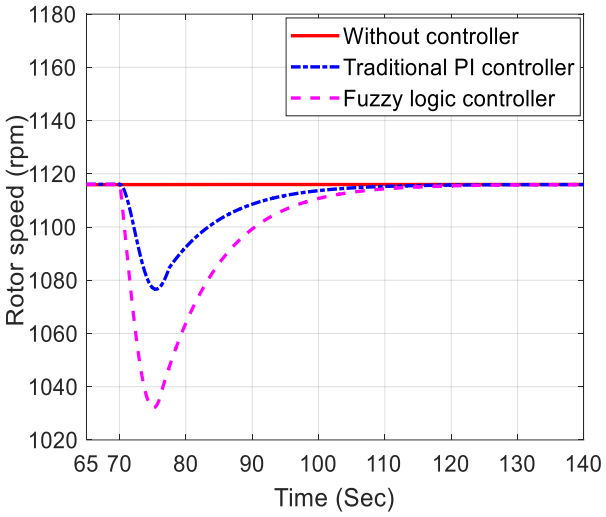


Fig 11. (b) Rotor speed at 9.3 m/s with 100 MW

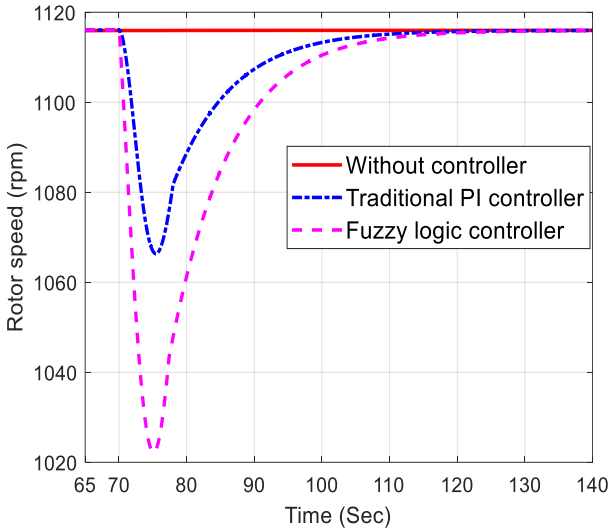


Fig 12. (b) Rotor speed at 9.3 m/s with 125 MW

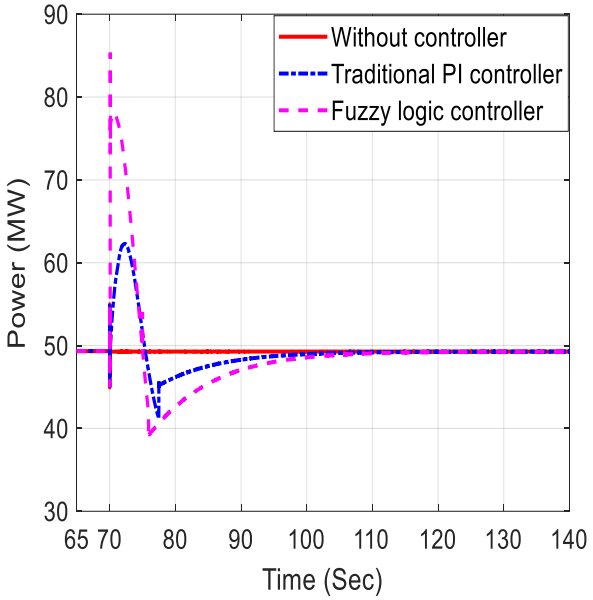


Fig 11. (c) Power at 9.3 m/s with 100 MW

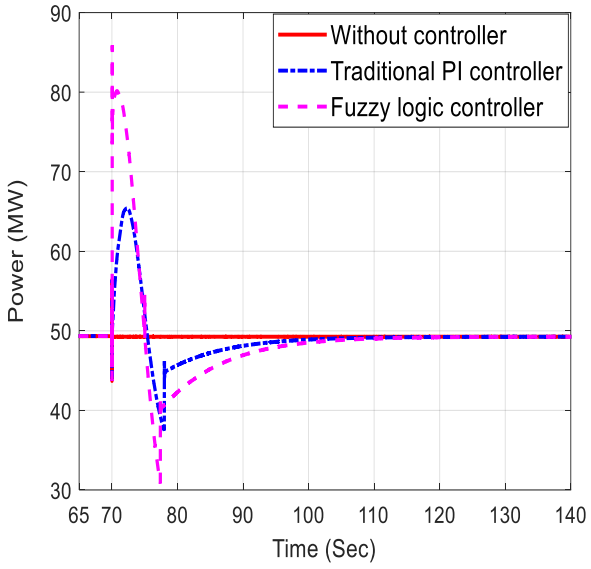


Fig 12. (c) Power at 9.3 m/s with 125 MW

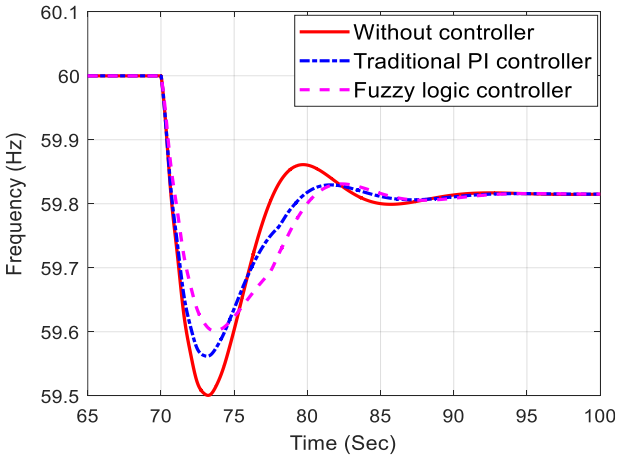


Fig 12. (a) Frequency at 9.3 m/s with 125 MW

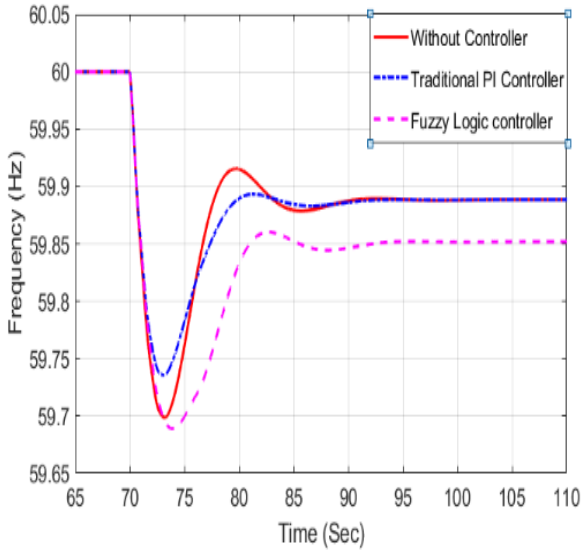


Fig 13. (a) Frequency at 10 m/s with 75MW

Volume: 12 Issue: 06 Pages: 4732-4741(2021) ISSN: 0975-0290

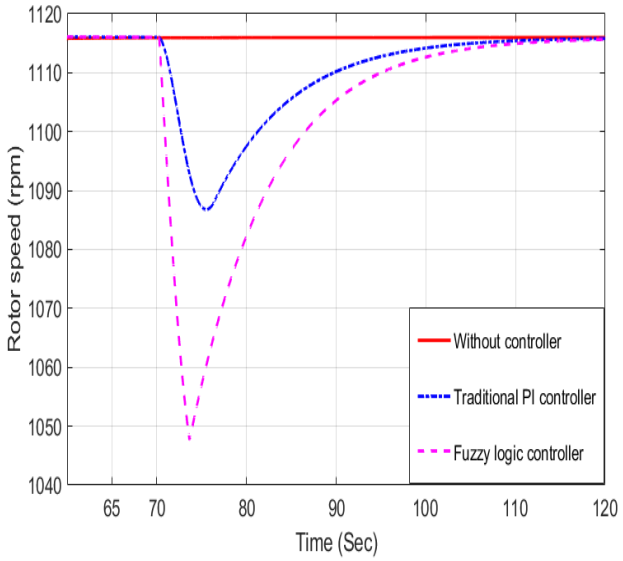


Fig 13. (b) Rotor speed at 10 m/s with 75MW

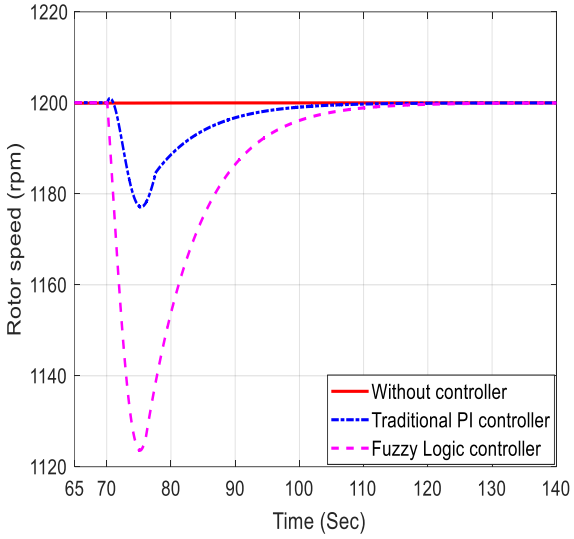


Fig 14. (b) Rotor speed at 10 m/s with 100 MW

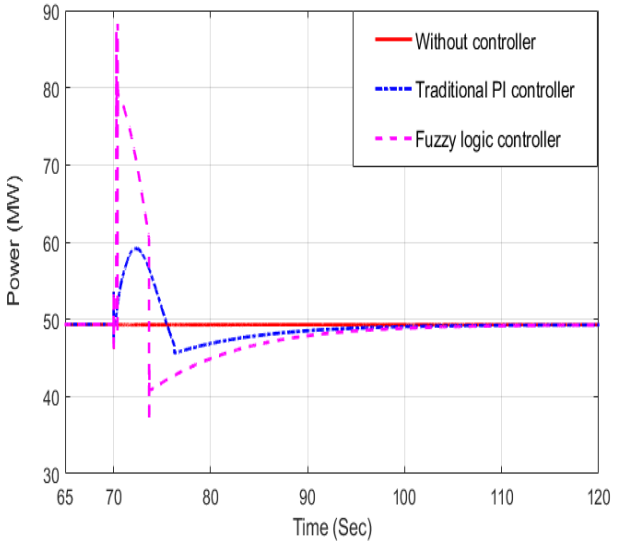


Fig 13. (c) Power at 10 m/s with 75MW

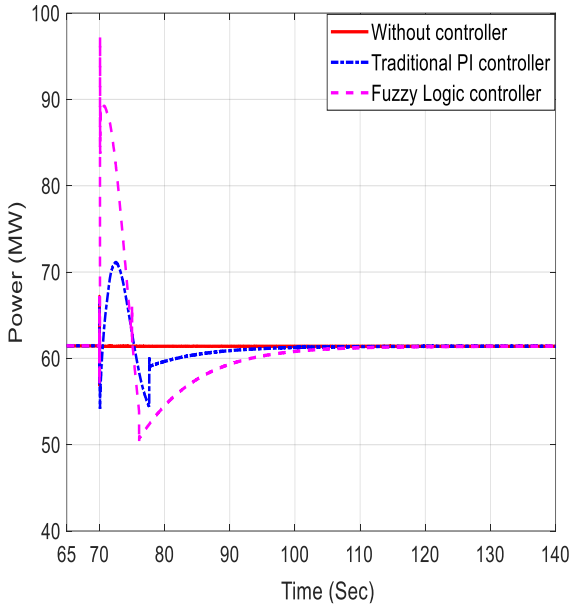


Fig 14. (c) Power at 10 m/s with 100 MW

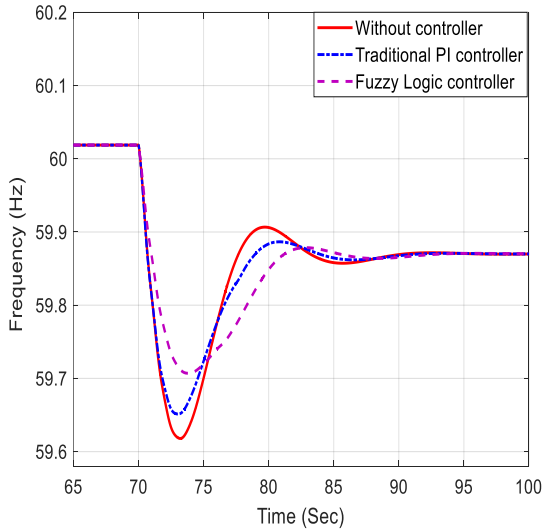


Fig 14. (a) Frequency at 10 m/s with 100 MW

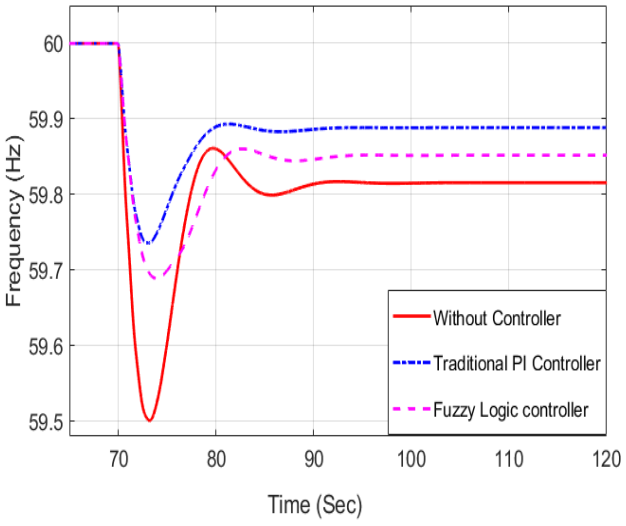


Fig 15. (a) Frequency at 100 m/s with 125 MW

Volume: 12 Issue: 06 Pages: 4732-4741(2021) ISSN: 0975-0290

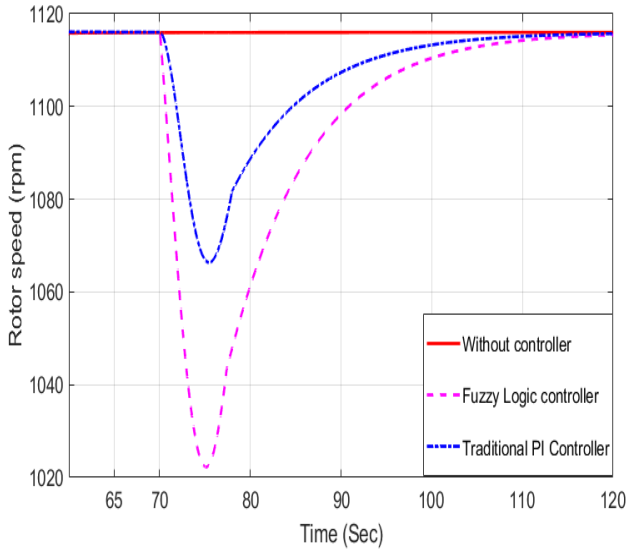


Fig 15. (b) Rotor speed at 10 m/s with 125 MW

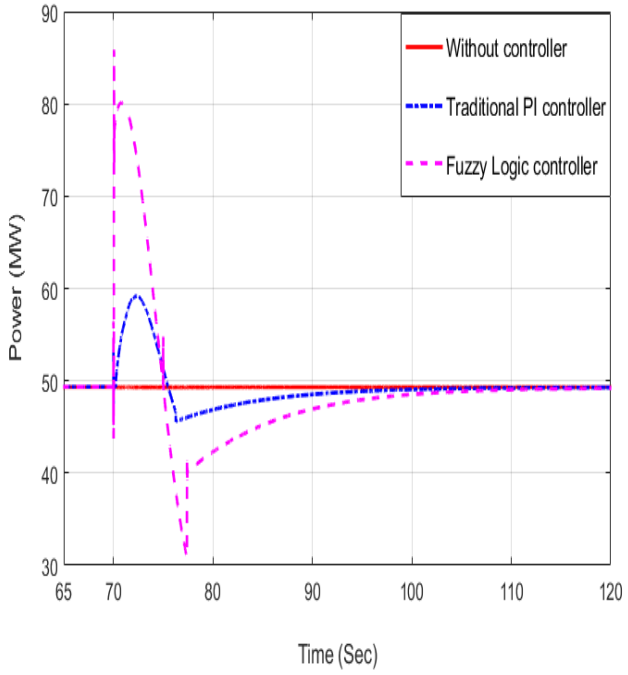


Fig 15. (c) Rotor speed at 10 m/s with 125MW

Both of the tests were carried out at various wind speeds and loads, and as seen in Fig.7-15, our suggested fuzzy logic controller system optimizes frequency faster and similar to the optimal frequency than other controllers. The suggested fuzzy logic controller approach has a stronger frequency regulation technique when combined with the inertia control variable coefficient. As seen in Fig.7-15, the frequency variance of our proposed approach is lower than that of current methods. We can monitor frequency regulation stability faster with the enhanced method than with other techniques.

## IV. CONCLUSION

We introduced a fuzzy logic controller approach that is integrated with a standard PI controller in this paper. The proposed approach enhanced the frequency regulation and frequency variance of standard PI controller-based frequency regulation. The without-controller system, the PI conventional method, and the proposed fuzzy logic controller method are both evaluated and contrasted. At high wind penetration, our proposed solution allows the device more reliable than conventional grid frequency, and there is no direct relationship between rotor speed and wind turbine frequency. After multiple iterations, the optimal set of fuzzy logic control coefficients (kd, kp) is assured to satisfy the frequency regulation requirements. Furthermore, the proposed scheme may be applied in real-time implementations without requiring any additional changes.

## REFERENCES

[1] Abdel-Khalik, A., Elserougi, A., Massoud, A., Ahmed, S., 2013. A power control strategy for flywheel doubly-fed induction machine storage system using artificial neural network. Electr. Power Syst. Res. 96, 267–276.

[2] Asl, H.J., Yoon, J., 2016. Power capture optimization of variable-speed wind turbines using an output feedback controller. Renew. Energy 86, 517–525.

[3] Datta R, Ranganathan VT. Variable-Speed Wind Power Generation Using Doubly Fed Wound Rotor Induction Machine - A comparison With Alternative Schemes. IEEE Transactions on Energy Conversion. 2002; 17(3): 414– 421.

[4] Li G, M Yin, M Zhou, C Zhao. Decoupling control for multi terminal VSCHVDC based wind farm interconnection. IEEE. Power Engineering Society General Meeting. 2007: 1-6.

[5] Holdsworth L, XG Wu, JB Ekanayake and N Jenkins. Comparison of fixed speed and doubly-fed induction wind turbines during power system disturbances. IEE Proc. Gener. Transm. Distrib., 2003; 150 (3): 343-352.

[6] Baloch, M.H., Wang, J., Kaloi, G.S., 2016. Stability and nonlinear controller analysis of wind energy conversion system with random wind speed. Int. J. Electr. Power Energy Syst. 79, 75–83.

[7] Balogun, A., Ojo, O., Okafor, F., 2013. Decoupled direct control of natural and power variables of doubly fed induction generator for extended wind speed range using feedback linearization. IEEE J. Emerg. Sel. Top. Power Electron. 1, 226–237.

[8] Katiraei F, MR Iravani and PW Lehn. Micro-Grid Autonomous Operation During and Subsequent to Islanding Process. IEEE Trans. Power Delivery. 2005: 20(1).

Volume: 12 Issue: 06 Pages: 4732-4741(2021) ISSN: 0975-0290

[9] Shaikh Jamshed Ali, Junjie Tang, Umer Farooq, Muhammad Shoaib Bhutta, Nouman Faiz, and Muhammad Umaid. "Innovative Frequency Regulation Strategies for DFIG based Wind Turbine Systems." In 2021 6th Asia Conference on Power and Electrical Engineering (ACPEE), pp. 794-798. IEEE, 2021.

[10] Reynolds MG. Stability of wind turbine generators to wind gusts. Purdue University Report TR-EE 79-20.

[11] Heier S. Grid integration of wind energy Conversion systems. Chichester: John Wiley and Sans Ltd. 1998; 35-302.

[12] Slaotweg G, H Polindcr, WL Kling. Dynamic modeling of a wind turbine with direct drive synchronous generator and back to back voltage source converter and its control. Proceedings of the European Wind Energy Conference, Copenhagen, Denmark. 2001; 1014-1017.

[13] Younis Rida, Amina Iqbal, Umer Farooq, Awais Iqbal, Habib Ullah Manzoor, Amir Mehmood, and Tareq Manzoor. "Techno-Economo-Environmental Viability Assessment of Grid-Connected Photovoltaic System-A Case for Different Cities of Pakistan." In 2018 International Conference on Power Generation Systems and Renewable Energy Technologies (PGSRET), pp. 1-5. IEEE, 2018.

[14] Bourdoulis, M.K., Alexandridis, A.T., 2014. Direct power control of DFIG wind systems based on nonlinear modeling and analysis. IEEE J. Emerg. Sel. Top. Power Electron. 2, 764–775.

[15] DENNISTON N, MASSOUD A M, AHMED S, et al. Multiple-module high-gain high-voltage DCDC transformers for offshore wind energy systems [J]. IEEE Transactions on Industrial Electronics, 2011

[16] IEEE. Terms, Definitions and Symbols for Subsynchronous Oscillations [J]. IEEE Power Engineering Review, 1985,

[17] MOHAMMADPOUR H A, SANTI E. Analysis of subsynchronous control interactions in DFIG- based wind farms: ERCOT case study [M]. 2015 IEEE Energy Conversion Congress and Exposition, ECCE 2015. 2015.

[18] FAN L, MIAO Z. Mitigating SSR using DFIG-based wind generation [J]. IEEE Transactions on Sustainable Energy, 2012,

[19] Ali Shaikh Jamshed, Poonam Lohana, Nouman Faiz, Umer Farooq, and Naqqash Ahmed. "Intelligent Frequency Control Strategy of Wind Turbine Generation System with DFIG by Using PI and Fuzzy Logic Controllers." (2020).

[20] M. K. Kim, "Optimal Control and Operation Strategy for Wind Turbines Contributing to Grid Primary Frequency Regulation," Appl. Sci., vol. 7, pp. 1–23, September 2017.

[21] Farooq Umer, Fan Yang, Yi Jun, Muhammad Arshad Shehzad Hassan, Nouman Faiz, Muhammad Tanveer Riaz, Li Jinxian, and Jamshed Ali Shaikh. "A Reliable Approach to Protect and Control of Wind Solar Hybrid DC Microgrids." In 2019 IEEE 3rd Conference on Energy Internet and Energy System Integration (EI2), pp. 348-353. IEEE, 2019.

[22] I. Kharchouf, A. Essadki, T. Nasser "Wind System Based on a Doubly Fed Induction Generator: Contribution to the Study of Electrical Energy Quality and Continuity of Service in the Voltage Dips Event," Int. J. Renew. Ener. Reas., vol. 7, no.4, pp. 1892-1900, December 2017.

[23] Farooq Umer, Habib Ullah Manzoor, Aamir Mehmood, Awais Iqbal, Rida Younis, Amina Iqbal, Fan Yang, Muhammad Arshad Shehzad Hassan, and Nouman Faiz. "Assessment of Technology Transfer from Grid power to Photovoltaic: An Experimental Case Study for Pakistan." International Journal of Advanced Computer Science and Applications (IJACSA) 10, no. 5 (2019).

[24] Y. Wang, G. Delille, H. Bayem et al., "High wind power penetration in isolated power systems-assessment of wind inertial and primary frequency response," IEEE Trans. Power Syst. 28(3), 2412–2420 (2013).

[25] S. Han and S. Han, "Development of short-term reliability criterion for frequency regulation under high penetration of wind power with vehicle-to-grid support," Electr. Power Syst. Res. 107, 258–267 (2014).

[26] Salahuddin Shaikh, Liu Changan, Maaz Rasheed Malik, "An Empirical and Comparatively Research on Under-Sampling & Over-Sampling Defect-Prone Data-Sets Model in Light of Machine Learning" International Journal of Advanced Networking and Applications - IJANA VOLUME 12, 2 Page No:4719-4724(2021)